Directivity enhancement and deflection of the beam emitted from a photonic crystal waveguide via defect coupling

Kaan Guven[1, 2] and Ekmel Ozbay[1, 2, 3]

[1]*Department of Physics, Bilkent University, Bilkent, 06800, Ankara, Turkey*
[2]*Nanotechnology Research Center, Bilkent University, Bilkent, 06800, Ankara, Turkey*
[3]*Department of Electrical and Electronics Engineering, Bilkent University, Bilkent 06800, Ankara, Turkey*
guven@fen.bilkent.edu.tr

Abstract: We experimentally and numerically investigate the spatial distribution of the emission from a photonic crystal waveguide, coupled with defects, that are located at the output edge. Two defects that are located symmetrically enhance the directivity of the beam compared to that of a plain waveguide, as was reported in recently conducted theoretical work. We further demonstrate that a single defect deflects of the beam. By choosing the defect resonance that is close to the edge of the pass band of the waveguide, where the group velocity of the beam within the waveguide is slow, a significant amount of deflection can be achieved.

OCIS codes: (160.4670) Optical materials; (260.5740) Physical Optics, resonance.

References and links

1. H. Kosaka, T. Kawashima, A. Tomita, M. Notomi, T. Tamamura, T. Sato, and S. Kawakami, "Self-collimating phenomena in photonic crystals," Appl. Phys. Lett. **74**, 1212 (1999).
2. S. Enoch, B. Gralak, and G. Tayeb, "Enhanced emission with angular confinement from photonic crystals," Appl. Phys. Lett. 81, 1588 (2002); S. Enoch, G. Tayeb, and B. Gralak, IEEE Trans. Antennas Propag. **51**, 2659 (2003).
3. D. N. Chigrin, S. Enoch, C. M. S. Torres, G. Tayeb, "Self guiding in two-dimensional photonic crystals," Opt. Express **11**, 1203 (2003).
4. A. Martinez, H. Miguez, A. Griol, and J. Marti, "Experimental and theoretical analysis of the self-focusing of light by a photonic crystal lens," Phys. Rev. B **69**, 165119 (2004).
5. K. Guven, E. Ozbay, "A plain photonic crystal for generating directional radiation from embedded sources," J. Opt. A **9**, 239 (2007).
6. A. F. Koenderink and W. L. Vos, "Light exiting from real photonic band gap crystals is diffuse and strongly directional," Phys. Rev. Lett. **91**, 213902 (2003).
7. E. Moreno, F. J. Garcia, and L. Martin-Morena, "Enhanced transmission and beaming of light via photonic crystal surface modes," Phys. Rev. B **69**, 121402 (2004).
8. P. Kramper, M. Agio, C. M. Soukoulis, A. Birner, F. Müller, R. B. Wehrspohn, U. Gösele, and V. Sandoghar, "Highly directional emission from photonic crystal waveguides of subwavelength width," Phys. Rev. Lett. **92**, 113903 (2004).
9. S. K. Morrison and Y. S. Kivshar, "Engineering of directional emission from photonic crystal waveguides," Appl. Phys. Lett. **86**, 081110 (2005).
10. I. Bulu, H. Caglayan, and E. Ozbay "Beaming of light and enhanced transmission via surface modes of photonic crystals," Opt. Lett. 30, 3078 (2005).
11. Chii-Chang Chen, T. Pertsch, R. Iliev, F. Lederer, and A. Tünnermann, "Directional emission from photonic crystal waveguides," Opt. Express **14**, 2423 (2006).
12. H. Kosaka, T. Kawashima, A. Tomita, M. Notomi, T. Tamamura, T. Sato, and S. Kawakami, "Superprism phenomenon in photonic crystals," Phys. Rev. B **58**, 10096 (1998).
13. T. Baba, "Photonic crystal light deflection devices using the superprism effect," IEEE. J. Quantum Electron. **38**, 909 (2002).
14. L. Wu, M. Mazilu, and T. F. Krauss, "Beam steering in planar-photonic crystals: from superprism to supercollimator," J. Lightwave Technol. **21**, 561 (2003).
15. K. Guven, K. Aydin, K. B. Alici, C. M. Soukoulis, and E. Ozbay, "Spectral negative refraction and focusing analysis of a two-dimensional left-handed photonic crystal lens," Phys. Rev. B **70**, 205125 (2004).
16. E. Özbay, and B. Temelkuran, "Reflection Properties and Defect Formation in Photonic Crystals," Appl. Phys. Lett., **69**, 743 (1996).

#85036 - $15.00 USD Received 9 Jul 2007; revised 24 Aug 2007; accepted 24 Aug 2007; published 29 Oct 2007

17. E. Özbay, G. Tuttle, R. Biswas, K. M. Ho, J. Bostak, and D. M. Bloom, "New double-etch geometry for millimeter-wave photonic crystals with a semi-tunable photonic band gap," Appl. Phys. Lett. **65**, 1617 (1994).
18. W. Smigaj, "Model of light collimation by photonic crystal surface modes," Phys. Rev. B **75**, 205430 (2007).
19. A. Faraon, E. Waks, D. Englund, I. Fushman, and J. Vučković, "Efficient Photonic Crystal Cavity-Waveguide Couplers," Appl. Phys. Lett. **90**, 073102 (2007).
20. J. Goh, I. Fushman, D. Englund, and J. Vuckovic, "Genetic optimization of photonic bandgap structures," Opt. Express **15**, 8218 (2007).

1. Introduction

The spatial control of electromagnetic emission from photonic crystal (PC) waveguides is important for various applications. The propagation within a PC and emission from the PC surface can be made directional by employing photonic bands with negative refracting or extremely flat dispersion properties [1-5]. It was demonstrated that a diffuse yet strongly directional emission is possible for frequencies that are near the photonic band edges. [6] However, the emission from a waveguide with an abruptly ending output shows, in general, poor directivity. Several studies have reported that by corrugating the surface of the PC at the waveguide output, the waveguide mode excites surface modes which then can be coupled to propagating modes of freespace, in order to form a directional beam. [7-10] A recent study proposes the coupling of a waveguide to defects at the termination in order to form an optical field distribution that is similar to that of a triple point source system, which can yield a beam with low angular divergence. [11] In addition to the beaming effect, the diverse dispersion of photonic bands leads to negative refraction (effective refractive index $n_{\text{eff}} < 0$) and the super-refraction ($0 < n_{\text{eff}} < 1$) phenomena, which can be utilized as beam deflection devices in photonic circuits [12-14].

It may also be desirable to have a beam deflection mechanism for the waveguide emission without placing a deflector element in front of the waveguide output. In the present paper, we discuss such a design based on a PC waveguide that is coupled with cavities at the output edge. We follow a recent theoretical work given in Ref. [11], where the authors demonstrate the directivity enhancement of PC waveguide emission via coupling to cavities at the output. We demonstrate that, while the symmetrically placed defects enhance the directivity, as was predicted in Ref. [6], a single defect can induce the deflection of the beam in certain direction. The amount of deflection depends on the resonance frequency of the defect. In particular, a defect resonance that is near to the transmission band edge provokes significant beam deflection.

The present paper is organized as follows. In Section 2, the PC structure is described and the transmission spectra of the waveguide and of the coupling defects are shown. The third section presents the main results of the study consisting of the simulated and measured angular resolved transmission spectrum of the waveguide which is coupled with defect(s). The last section concludes the paper.

2. Description of photonic crystal and defects

The 2D photonic crystal used in the present study is a hexagonal lattice of alumina rods. The relevant crystal parameters are as follows. The alumina rods have a diameter of $2r = 3.1$ mm, and a dielectric constant of $\varepsilon = 9.8$. The lattice constant is $a = 7.0$ mm. The rods are 150 mm long. In the experiment, the out-of-plane radiation is blocked by microwave absorbers. In the simulations, the PC has translational invariance in the direction parallel to the rods, in order for the system to be treated as purely two dimensional. We only investigated the propagation of TM polarized electromagnetic waves, where the electric field vector is parallel to the rods (following the convention in the field of photonic crystal).

We used a finite-difference-time-domain solver software (Rsoft-Fullwave) for simulating the PC structure. The PC has 41 layers in the ΓK direction and 21 layers in the ΓM direction. The waveguide is formed by removing one layer of rods along the ΓK direction. Figure 1 shows the PC structure for measuring the resonance frequency of the individual defects that are located within the waveguide (left panel).

#85036 - $15.00 USD Received 9 Jul 2007; revised 24 Aug 2007; accepted 24 Aug 2007; published 29 Oct 2007

The transmission spectra of the bare waveguide and the defect inserted waveguide that were obtained from (a) an experiment and (b) a simulation are shown in Fig.1 (right panel). The photonic band gap of the crystal is between 12.2 GHz, 19.2 GHz. The transmission band of the waveguide (WG) extends from 14.8 GHz - 18.8 GHz. In photonic crystals the defect mode can be identified as a highly confined mode within the transmission spectrum. [16]

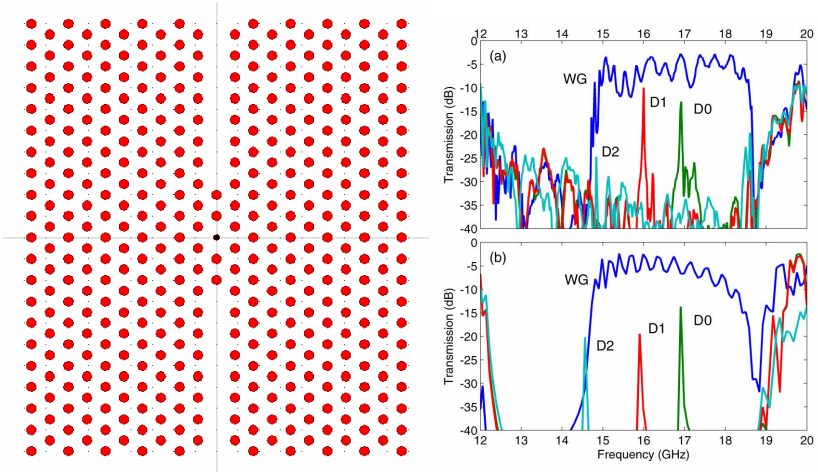

Fig. 1. (color online) **(left)** Schematic view of the PC-waveguide structure with a defect located at the center. This setup is used to measure the resonance frequency of the defects. **(right)** The (a) measured and (b) simulated transmission spectra of the waveguide, and the defects of radii r = 0, (D0), r = 505 μm (D1), and r = 760 μm (D2), respectively. The band gap of the 2D bulk photonic crystal extends from 12.2 GHz - 19.2 GHz.

The defects (D0, radius r = 0, D1, r = 505 μm and D2, r = 760 μm) exhibit resonance modes with measured frequencies, f_0 = 16.92 GHz, f_1 = 16.00 GHz, and f_2 = 14.82 GHz. The respective resonance frequencies obtained from the simulations are f_0 = 16.92 GHz, f_1 = 15.90 GHz, and f_2 = 14.57 GHz. The slight displacement of the rods at and around the defect location can obviously induce a noticeable change in the observed resonance frequency, which is the main reason for the difference between measured and simulated results, particularly for the larger defect (D2).

3. Angular resolved transmission spectrum of the defect coupled waveguide structure:

In the experiment, a single detector antenna attached to a swinging arm is used to measure the polar distribution of the waveguide emission in 2.5 degree steps. The distance between the aperture of the detector antenna and the output surface of the waveguide is 780.0 mm which is approximately half of the distance for the far field zone $2d^2/\lambda$ (d being the width of the emitting surface). Since, the radiation profile is mainly determined by the local region containing the waveguide output and the defect, this distance qualitatively accounts for the radiation zone as well. The input signal to the waveguide is provided by a horn antenna at the other end. The signal is swept in 12 GHz - 18 GHz in 400 steps, using an averaging factor of 32 at each step. The simulation employs a set of 37 monitors that are distributed in 5 degree steps along a semicircle, at a radius of 30a away from the waveguide termination [Fig. 2(a)]. For the spectral analysis, an electromagnetic pulse is sent through the waveguide and the transmitted signal is recorded by the monitors. The Fourier transform of the signal gives the transmission spectrum. Figure 2(a) shows a CW simulation at the resonance frequency of the defect, which will be discussed further below. The defect(s) are located $a\sqrt{3}$ away from the waveguide axis. Figure 2(b) shows a single defect (alumina rod with a smaller radius) located on the left side of the waveguide termination.

#85036 - $15.00 USD Received 9 Jul 2007; revised 24 Aug 2007; accepted 24 Aug 2007; published 29 Oct 2007

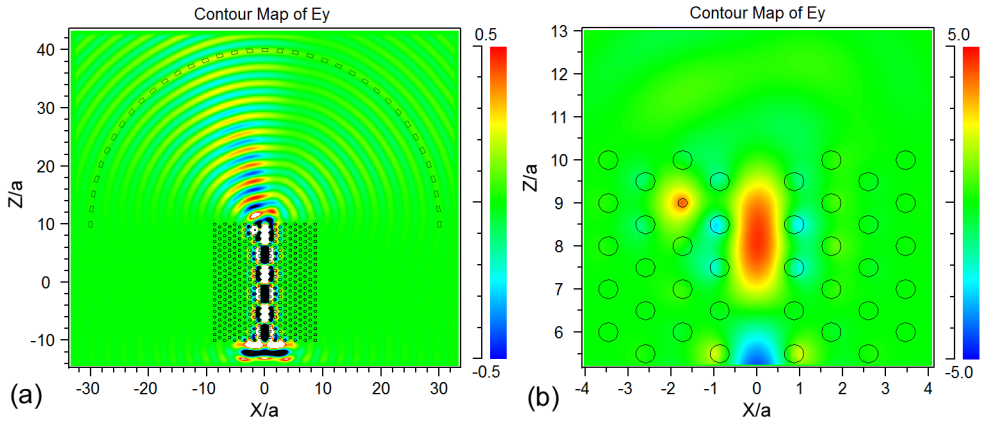

Fig. 2. (color online) (a). Schematic view of the simulated PC-waveguide structure with a defect located at the left edge of the output, and an array of field monitors placed along the semicircle. The input signal propagates upwards through the waveguide. (b). Detailed view of the waveguide end and the coupling defect.

The transmission spectrum of the plain waveguide (i.e. no coupling defects) is obtained as a reference. Figures 3(a) and 3(b) show the plain waveguide spectrum obtained from experiment and simulation. As expected, the angular confinement of the beam profile is loose, that is narrowing slightly towards the upper edge of the transmission band due to the decreasing wavelength. The maxima in the transmission spectrum are well known as the spectral splitting of the Fabry-Perot resonances due to the coupling between the cavities building the waveguide. The number of maxima is therefore proportional to the number of cavities that are building the waveguide. [18] Figure 3(c) is the polar plot of the beam profile taken at f = 17.2 GHz. The main beam is accompanied by two large sidelobes.

Figures 3(d) and 3(e) show the angular resolved transmission spectrum of the waveguide that is coupled with two cavities at the output. Close to f = 17 GHz, strong suppression of the sidelobes is noticeable from the colormap. The polar plot at f = 17.2 GHz shows that the angular confinement of the beam has improved, in agreement with Ref. 11. This frequency differs slightly from the frequency of the isolated defect resonance that was reported in section 2, but this was mainly due to the experimental error: The photonic crystal is constructed by inserting the dielectric rods into the holes in a plastic base. Inevitable yet small displacements of the rods between different measurement sessions can cause fluctuations in the observed resonance frequency, as it is highly sensitive to such disorders.

#85036 - $15.00 USD Received 9 Jul 2007; revised 24 Aug 2007; accepted 24 Aug 2007; published 29 Oct 2007

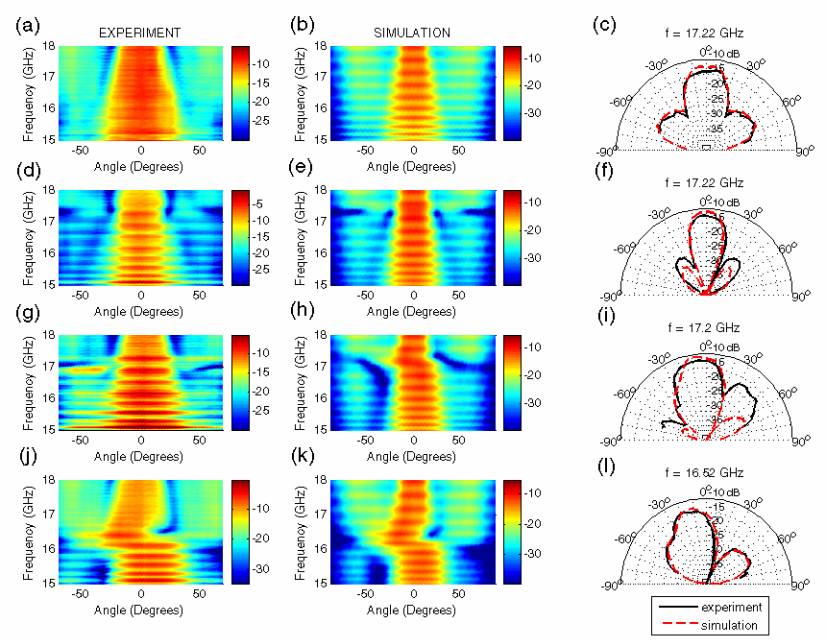

Fig. 3. (color online) The angular resolved transmission spectra of: (a-c) plain waveguide, (d-f) waveguide + two D0 defetcs, (g-i) waveguide + single D0 defect, (j-l) waveguide + single D1 defect. The last column shows the experimental (solid) and simulated (dashed) polar plot of the beam profile at 17.2 GHz (c,f, and i) and at 16.5 GHz (l) taken from their respective spectrum.

Next, the angular resolved transmission spectra for the waveguide coupled with single defect D0 [Fig. 3(g), 3(h)] and D1 [Fig. 3(j), 3(k)] are shown. The single defect causes a deflection of the beam around its resonance frequency. The deflection occurs towards the side where the defect is located. However, the enhancement of directivity is lost. The polar profiles deviate only for the sidelobe transmission level for C0 but this is due to the slight change in the resonance frequency of the defect for this measurement. We kept the "plot" frequency fixed instead of providing a better fitting profile close to but different than 17.2 GHz.

The time averaged angular transmission is plotted in Fig. 4(a) for the bare waveguide and the waveguide + 2D0 structures. It can be concluded that the presence of the cavities result in a strong suppression of the sidelobe emission from the waveguide. In addition, slight enhancement (~3 dBm) of the beam along the propagation axis is observed. In Figure 4(b), we plot the polar profiles of the beam that is emitted by the defect coupled waveguide, at the respective defect resonance frequency. These results are obtained from simulations. In addition to the experimentally available defect sizes, we simulated a defect which exhibit resonance at the lower edge of the waveguide transmission band. The polar profiles indicate that the amount of deflection increases as the defect frequency is located closer to the transmission band edge. For the defect at the band edge, the deflection is approx. 20^{o}. The asymmetric profiles exhibit a side lobe as well, but these remain approx. 12 dBm below the main beam intensity. The defect-waveguide coupling depends on the overlap of their respective spatial mode distributions. The waveguide has dispersion and the spatial distribution of the waveguide mode is different for different frequencies. It is fair to assume that the defect mode remains Gaussian shaped, hence, the observed deflection rather depends on the change in the spatial distribution of the waveguide mode.

The collimation of the electromagnetic wave emitted by PC waveguides was described by a model based on the surface modes of the PC qualitatively [7-10], and recently quantitatively [18]. In the case of a defect-waveguide system, a similar formulation may be developed to

#85036 - $15.00 USD Received 9 Jul 2007; revised 24 Aug 2007; accepted 24 Aug 2007; published 29 Oct 2007

describe the optical field for which the spatial and spectral properties are mainly by way of three components: the waveguide, the coupling defect(s) and the surface of the photonic crystal. The defect essentially acts as another radiating source and alters the optical field that is solely generated by the waveguide, in turn resulting in a deflection of the beam profile. The directivity of the deflected beam can also be improved by using surface corrugation along the PC surface around the waveguide output [10]. The defect-waveguide coupling can be improved [19], and multimode cavities can be employed resulting in different deflection properties

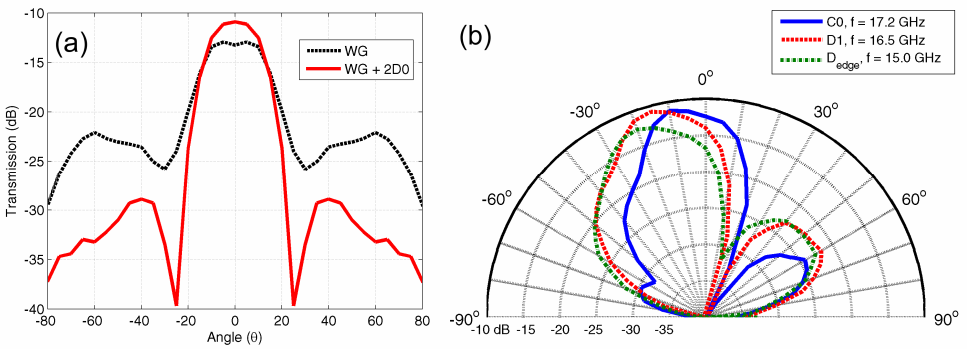

Fig. 4. (color online) (a). The time averaged angular transmission profile for the bare waveguide and the waveguide coupled with two defects (D0). (b). The polar plot of the beam for different defects at their respective resonance frequencies.

4. Conclusion

We demonstrated experimentally that the sidelobe suppression and the deflection of the waveguide emission can be achieved using defects. The optimization of the defect-waveguide system can be performed by genetic algorithms [20] according to the particular specifications. In this study only the simple cavity mode is considered. This can be extended for multimode cavities with different mode profiles, where different radiation patterns can occur. A further extension might be to incorporate a tunable defect so that the resonance frequency can be changed within the transmission band of the waveguide. Active materials can be used to change the dielectric constant of the defect by way of photoexcitation or by a locally applied electric field. In this context, the use of three-dimensional PC with defect-waveguide coupling can also give interesting results. [17]

In conclusion, the present work demonstrates that the PC waveguide coupled to defect(s) at the output may provide a basic template for modifying the spatial distribution of the waveguide emission, which can be utilized in microwave and photonic applications.

Acknowledgments

This work is supported by the European Union under the projects EU-NoE-METAMORPHOSE, EU-NoE-PHOREMOST, and TUBITAK under the Project nos. 104E090, 105E066, 105A005, and 106A017. One of the authors (E.O.) also acknowledges partial support from the Turkish Academy of Sciences.

#85036 - $15.00 USD Received 9 Jul 2007; revised 24 Aug 2007; accepted 24 Aug 2007; published 29 Oct 2007